

Predicting and Applying Wellhead Temperatures for Steamflood-Field Operation and Production-Performance Monitoring

Zhengming Yang, Aera Energy LLC

Summary

Producer-flowline temperatures (FLTs) can be measured automatically with a thermistor on an emergency-shutdown system (ESD), or manually on a specified spot on flowline with a handheld unit. Measured FLTs can usually be mapped to represent the formation-temperature distribution for steamflood reservoir management purposes (Hong 1994; Nath et al. 2007). In addition to FLT, wellhead temperature (WHT) is another surface temperature. Predicting the long-term WHT trend in steamflood operation is necessary for designing surface facilities for both oil dehydration/separation and produced-water recycling. This predicted temperature will also be applicable for production-performance monitoring.

To predict the wellhead temperature, Hasan et al. (2009) derived a steady-state analytical solution for calculating WHT from bottom-hole temperature (BHT) under flowing conditions of a multisection slant wellbore for the isothermal primary-depletion process, with both WHT and BHT being time independent for a given gross rate (Igec et al. 2010). This steady-state analytical solution has been extended to calculate steamflood producer WHT from BHT (both are time dependent) by consecutively approximating the WHT and monthly average of FLT measurements to a steady-state solution. The monthly averaged FLTs are seasonally variable and higher in the summer months of July through September and lower in the winter months of December through February. Monthly averaged FLT measurements depend on an annual ambient-temperature cycle within the depth needed for reaching an undisturbed ground temperature (typically 30 to 50 ft) (Gwadera et al. 2017). WHT, if measured, should be comparable with FLT for their close typical distance of 5 to 10 ft. WHT prediction, however, is only process dependent and not seasonally variable because of the inability to describe seasonally undisturbed depth in the geothermal gradient. Therefore, WHT prediction can be validated with average summer-month FLT measurements when heat loss becomes minimal. BHTs in this analytical approach are predicted by the Lauwerier (1955) analytical model and improved by calibration with the available reservoir-simulation model or several years of FLT measurements for steamflood response time.

The objective of this study is to develop an integrated production-monitoring approach using only the surface information, including WHT and FLT, oil/water-production rate, and injection-pressure/rate data, which can be applied to diagnose and optimize steamflood production performance. A field case study for the South Belridge Diatomite steamflood was investigated. WHT prediction is compared with FLT measurement for diagnosing and understanding the production performances, such as premature water or steam breakthrough, interference by the waterflood on the steamflood boundary producers, as well as the FLT variation related to the target rates for steam injection. This diagnostic analysis approach combined with the Buckley-Leverett theory-based displacement-efficiency analysis, and injection pressure and rate signal, will help to develop an improved understanding of the displacement detail and form a decision base to optimize the production performance.

Introduction

Temperature is an important process parameter for steamflood reservoir management, which can be measured either in situ (downhole) or at surface flowline. In-situ temperature measurements include fiber-optics distributed-temperature sensing installed on producers or observation wells to monitor the steam-breakthrough zone. However, with limited observation wells in a commercial steamflood-development project, as well as the variation of temperature measurement on a producer wellbore (because of pumpon/pumpoff operational cycles), and the phasing out of fiber optics with time, the in-situ temperature information is generally insufficient to monitor the field-steamflood operation. On the other hand, FLTs can be acquired easily and are abundant. Producer FLTs can be measured automatically with a thermistor on the flowline of an ESD, or manually with a handheld unit on a specified flowline spot.

FLT measurements were traditionally applied to monitor the steam-zone development by mapping its areal distribution (Hong 1994). In this study, the application of FLT data from its temporal trend with a maturing steamflood process on an individual producer or area basis will be investigated. In this regard, a predicted temperature trend is needed to compare and interpret FLT measurements into understanding the steamflood production performance. The nearest temperature to FLT in the production-operation system is the WHT. FLT depends on WHT and heat transfer in the surface-pipeline section. WHT depends on BHT, gross-flow rate, and producer-wellbore heat-transfer conditions. BHT depends on the formation heating from steam injection. To avoid involving unnecessary over-detailed daily ambient-temperature variation of diurnal/nocturnal cycles, monthly averaged FLT is applied, which is the monthly average of daily averaged FLT measurements. FLT is seasonally variable, and higher in the summer months of July through September and lower in the winter months of December through February. The seasonal variation of FLTs is attributed to the surface pipeline (5 to 10 ft from wellhead) and ground depth (30 to 50 ft) needed to reach the undisturbed geothermal gradient (Gwadera et al. 2017). WHT, if measured, should be comparable with FLT for their close distance and might not provide much additional assistance to production-performance monitoring. The predicted WHTs depend on production rates, BHTs, and wellbore-heat-transfer conditions, which are only process dependent and more valuable for the application of production-performance monitoring as an expectation to a long-term steamflood trend. WHT could be predicted in a reservoir simulation, like BHT, by taking each producer/wellbore heat transfer to the surface and taking the pump-operating condition into consideration, although such a modeling approach is inconvenient and

unnecessarily complicated, especially for the irregular overburden-formation-temperature profile caused by steamflood in the shallow Tulare Formation in South Belridge Diatomite Field (Dietrich 1990). To facilitate application for the practical field condition, an analytical WHT-prediction approach is preferred over reservoir simulation. An integrated two-step analytical approach is pursued in this study from BHT to WHT: BHT can be predicted using a model for reservoir heating and WHT can be predicted using a wellbore-heat-transfer model from BHT.

The case studies are for the **South Belridge Diatomite**, which is a 1,600-ft-thick, low-permeability, high-porosity reservoir including the Opal-A Formation (porosity of 50 to 60%) on the top and the Opal-CT Formation (porosity of 40 to 50%) below. Hydraulically induced fractures in both injectors and producers are required. Primary production started in 1977 for both the Opal-A and the Opal-CT formations. Waterflood and steamflood have been used to process the Opal-A Formation. Waterflood commercial development started in 1987, followed by commercial steamflood development in 2005. Vertically, there are five subsurface conformance intervals that are vertically isolated between depositional cycles. Producers are completed and commingled across all five cycles. Waterflood recovery remains in the flank areas. In the steamflood area, water injection is used in the uppermost cycle, primarily to serve as buffers and keep steam contained to the steam injection intervals. **Fig. 1** shows the steamflood pattern and injection strings. Displacement from the injector fracture to the producer fracture is linear flow (spacing 107.5 ft). Among the five injection strings, the water-injection string G is typically plugged back from the original water injector, and four steam injection strings (A, B, C, and D) are completed in two dual-tubing wellbores (A/B dual and C/D dual) to mechanically control the steam conformance profiles. Vertical communication between diatomite intervals can be ignored.

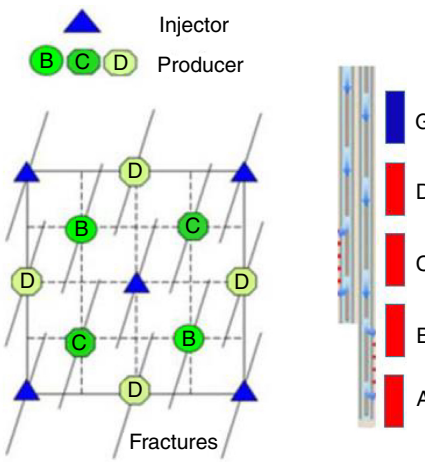


Fig. 1—Schematic of steamflood pattern and injection strings in South Belridge Diatomite.

BHT is the starting temperature of the wellbore heat transfer, WHT, and FLT. The traditional analytical/empirical “steam override” model by Neuman (1985) is only for the post-breakthrough steamflood-performance estimation and does not provide BHT calculation, besides the inappropriateness of the “steam override” model to this field. For formation-temperature calculation, in addition to the reservoir-heating model of Marx and Langenheim (1959), the Lauwerier (1955) convective/conductive formation-heat-transport model is straightforward. BHT can be calculated from the formation temperature at the producer location. To improve the representation of BHT, it is necessary to calibrate BHT from the Lauwerier (1955) model to BHT from reservoir simulation or to calibrate WHT (using the BHT and wellbore-heat-transfer model) to FLT measurements with the steam response time in the Lauwerier (1955) model.

WHT is predicted from BHT [from the Lauwerier (1955) model] in a steady-state wellbore-heat-transfer model by Hasan et al. (2009). The Hasan et al. (2009) steady-state wellbore-heat-transfer model was originally proposed for an isothermal primary-depletion process where both BHT and WHT are time independent for a given gross rate. In this study, it is extended to the thermal process of steamflood where both BHT and WHT are time dependent by consecutively approximating the WHT and monthly average of FLT measurements to a steady-state solution. One important feature in this steady-state wellbore-heat-transfer model is the multiple wellbore inclination and geothermal gradients from vertical to horizontal wells. This multiple geothermal gradient section applies to the complex overburden-temperature gradient attributed to steamflood in the Tulare Formation (Dietrich 1990). **Fig. 2** shows a temperature profile from the new producers. Only the Diatomite section follows the geothermal gradient ($g_G = 0.024^\circ\text{F}/\text{ft}$), with $T_{e0} = 73.134^\circ\text{F}$ at the surface and $T_e = T_{e0} + g_G D$ at depth D . A three-section formation-temperature-gradients model is needed to describe the overburden temperature, as shown in Fig. 2.

In the field case study, the analytically predicted BHT or WHT are calibrated with BHT (from reservoir simulation) or FLT measurements for determining steam response time, a parameter in the Lauwerier (1955) model. The steam response time depending on formation thickness, injector to producer spacing, and steam injection rate, as a consistent process parameter, can be applied to predict BHT in similar settings. With several years of FLT measurements during steamflood operation, this integrated analytical approach can be applied to practical field application when reservoir-simulation models are not available. A field case study was investigated with WHT prediction and monthly averages of FLT measurements. WHT prediction is compared with FLT measurement for diagnosing and understanding the production performances, such as premature water or steam breakthrough, interference by the waterflood on the steamflood boundary producers, as well as the FLT variation related to the target rate for steam injection. This diagnostic analysis approach, combined with the Buckley-Leverett theory-based oil cut/Y-function method for displacement efficiency investigation and injection pressure/rate signals in the producer-centered pattern analysis, will help to develop an understanding of the displacement detail and form a decision base to optimize the production performance. The field case study indicates the usefulness of this production-monitoring approach in steamflood-performance surveillance and optimization.

Methodology

The production-monitoring approach in this study only uses surface information, including temperature at producer wellhead (WHT) and flowline (FLT), injection pressure/rate, and oil/water production rates. Injection rate and pressure can be directly used as signals for

events correlation between injector(s) and producer(s). The Hall plot method can be applied to interpret the injectivity variation (Silin et al. 2005; Qi et al. 2017). The Y -function method, a Buckley-Leverett displacement-theory-based waterflood analytical solution, is applied to diagnose oil cut data for displacement efficiency. WHT and FLT are applied to understand the steamflood displacement condition in the formation.

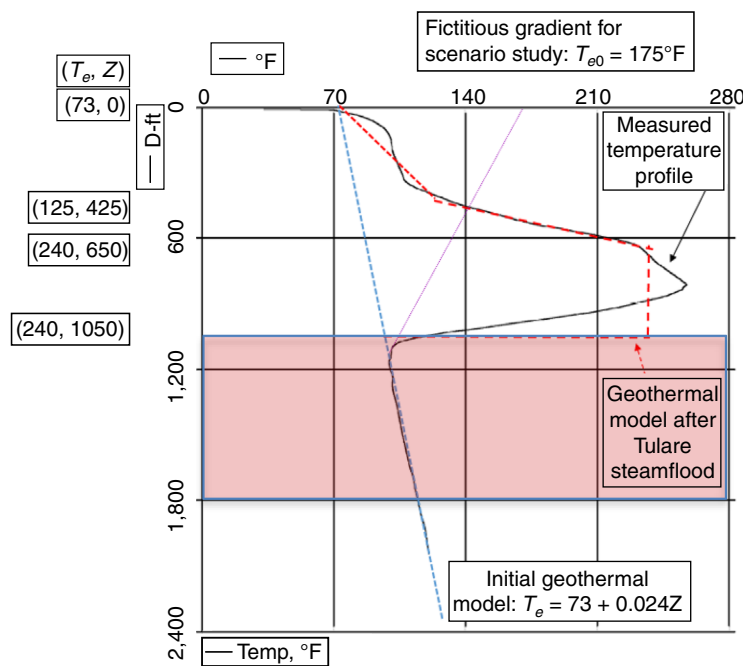


Fig. 2—Typical formation-temperature profile in South Belridge Field. Formation-overburden temperature is represented by a three-section formation-temperature gradient.

Temperature Prediction. Temperature data involved include FLT, WHT, and BHT. FLT is automatically measured when a producer-ESD system is installed or can be measured by a handheld unit on a specified spot on the flowline. WHTs are predicted from BHTs in the steady-state wellbore-heat-transport model (Hasan et al. 2009). BHT, representing steamflood formation heating in the wellbore-heat-transfer model, is typically obtained by modeling rather than direct measurement. BHT can be predicted in reservoir simulation using the steamflood operation policy. BHT history can be obtained from history matching the FLT data in the wellbore-heat-transfer model. Reservoir simulation is only used to validate the production-performance monitoring approach and is not an essential part of the practical field application.

BHT Prediction. Reservoir-simulation models were developed in some area in the South Belridge Diatomite Field for investigating waterflood optimization and steamflood development strategies (Yang and Urdaneta 2017). In CMG STARS™ reservoir simulator (Computer Modelling Group, Calgary, Alberta, Canada), the BHT can be obtained by defining a “sector” containing all gridblocks within producer-perforation intervals.

BHTs can also be analytically modeled using the Lauwerier (1955) convective/conductive formation-heat-transport model, which is a 2D and two-layer system, as shown in **Fig. 3**. The dimensionless formation temperature is shown in Eq. 1, which has an approximate analytical form (see Appendix A for details),

$$\frac{T_1 - T_r}{T_s - T_r} = \operatorname{erfc}\left(\frac{\xi}{2\sqrt{\theta(\tau - \xi)}}\right)U[\tau - \xi], \quad \dots \dots \dots \quad (1)$$

where the dimensionless variables are time $\tau = \lambda_2 t / (b^2 \rho_1 c_1)$, distance $\xi = x \lambda_2 / (b^2 \rho_w c_w v_w)$, and the heat-capacity ratio $\theta = (\rho_1 c_1) / (\rho_2 c_2)$ between the formation and the overburden. Linear velocity v_w , which is fracture spacing (107.5 ft) divided by time-to-response (in years), is a key process parameter.

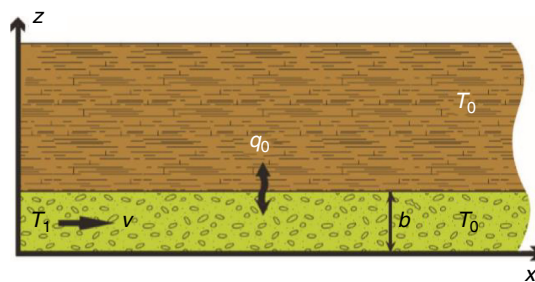


Fig. 3—Schematic for Lauwerier (1955) model (after Saeid and Barends 2009).

BHTs at different times can be obtained at the producer end (well spacing = 107.5 ft, as shown in Fig. 4a). Fig. 4b compares average BHTs from the reservoir simulation of the 2008 project and the Lauwerier (1955) model by adjusting the steam response time. A response time of 1.59 years in the Lauwerier (1955) model can reasonably and for the most part represent the BHT in reservoir simulation, which verifies the appropriateness of applying the BHT from the Lauwerier (1955) model in the analytical approach. The difference will be discussed in detail later.

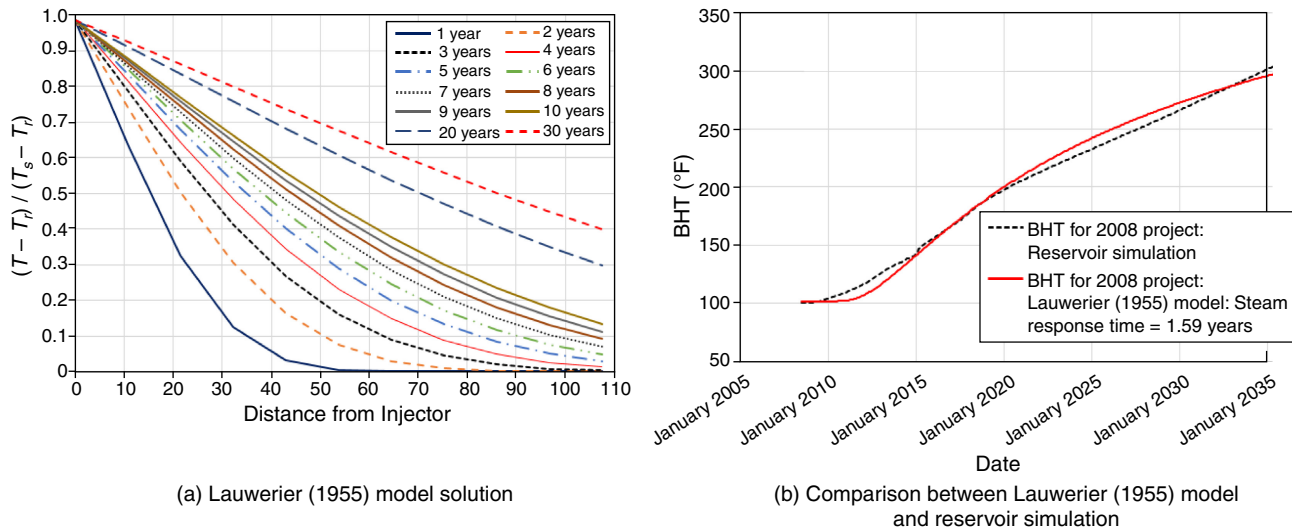


Fig. 4—Calibrate BHTs from (a) the Lauwerier (1955) formation-temperature solution and (b) reservoir simulations with steam response time.

WHT Prediction. Reservoir simulation only models the reservoir section for BHT without the wellbore in the overburden formations for WHT. CMG STARS reservoir simulator has the SAMODEL feature designed for injector/wellbore-heat-loss calculation. For characteristic investigation into the producer/wellbore heat transfer to both waterflood and steamflood, a producer is modeled as an injector with BHT reversed as the injection-water temperature at top, with 105°F for waterflood and 350°F for steamflood, assuming formation temperature of 105°F at 1,000-ft depth and 175°F on the surface. Fig. 5 demonstrates the transition of temperature from transient to steady state. For both waterflood (BHT = 105°F) and steamflood (BHT = 350°F), the model WHT changes slowly after the first month, which justifies the validity of applying the steady-state wellbore-heat-transfer model. The monthly averaged FLT will be used in the steady-state wellbore-heat-transfer model for this reason.

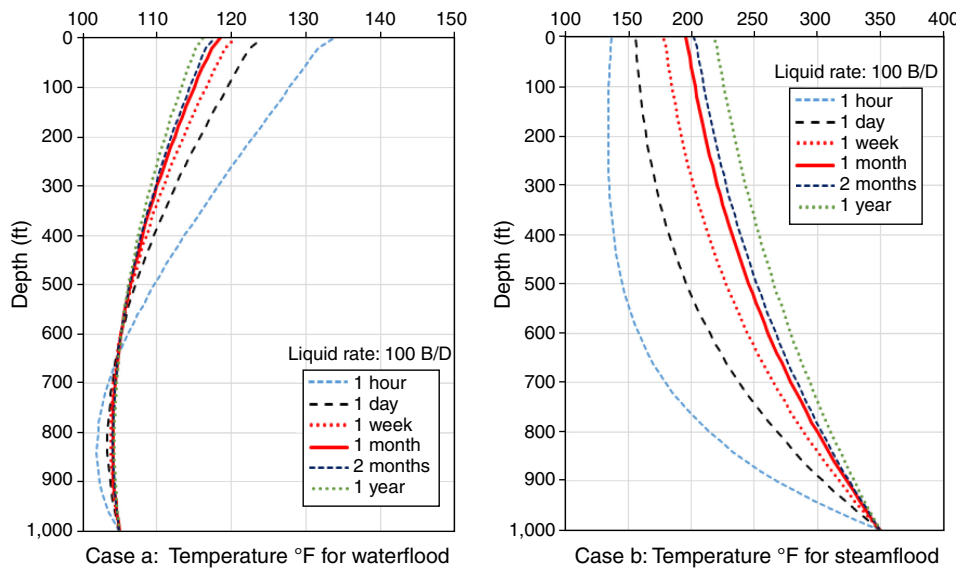


Fig. 5—Wellbore temperature of production fluid: transient- to steady-state transition.

Hasan et al. (2009) proposed an analytical solution for a steady-state wellbore heat transfer for both injectors and producers with multiple wellbore inclinations and geothermal gradient sections. The steady-state solution of WHT (T_{fWH}) has a linear relationship with BHT (T_{fBH}) for the three-section formation-temperature-gradient representation to overburden temperature (Fig. 2) in the South Belridge Diatomite (see Appendix B for details).

$$T_{fWH} = A \cdot T_{fBH} + B, \quad \dots \dots \dots \quad (2a)$$

with slope A and intercept B depending on formation depth D , formation-temperature gradient g_G , and wellbore-heat-transfer steady-state relaxation parameter L_R ,

$$B = T_{eWH} - T_{eBHE} e^{-DL_R} + \frac{1 - e^{-z1L_R}}{L_R} g_{G1} + \frac{e^{-z1L_R} - e^{-z2L_R}}{L_R} g_{G2}. \quad \dots \dots \dots \quad (2c)$$

Y-Function Method for Displacement-Efficiency Analysis. For waterflood with an unfavorable mobility ratio, Yang (2009, 2012) developed an analytical method to diagnose production performance and to forecast the oil-production rate,

where f_o is the oil fractional flow (oil cut); B is a constant in the expression $k_{ro}/k_{rw} = Ae^{-BS_w}$ (where S_w is water saturation; k_{ro} and k_{rw} are oil and water relative permeabilities, respectively; and A is a constant); E_V is the volumetric sweep efficiency; PV is the total pore volume (PV) (in bbl) in the subject area; and Q_L is the cumulative liquid production (in bbl). The group parameter $(E_V/B)PV$ can be obtained from historical production data and it is unnecessary to determine individual parameters unless the purpose is to calculate volumetric sweep efficiency.

Although its basis is waterflood, the Y -function method is useful in qualitatively analyzing steamflood production performance for the oil-banking effect, the displacement efficiency variations caused by steam channeling, as well as the interference on the boundary between these two recovery processes (Yang 2012). The schematic flow-regime diagram in Fig. 6 was applied to diagnose the oil cut/ Y -function into understanding on the displacement efficiency.

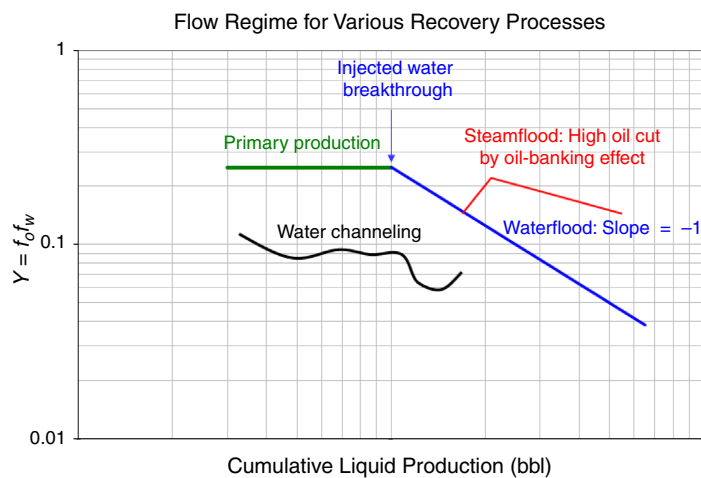


Fig. 6—Flow regime for production-performance diagnosis with Y-function method.

The workflow of this production-monitoring approach is described here. We first compare WHT prediction as an indication for a normal steamflood-maturity trend with FLT measurements to diagnose possible abnormal behaviors; then use the Y -function method to examine the possible effect on the displacement efficiency; and correlate injector and producer events and suggest a decision base for production-performance optimization.

Field Case Study

The field case study predicts and validates BHT and WHT to the South Belridge Diatomite steamflood and demonstrates the application of a production-monitoring approach in steamflood operation.

Case 1: Predicting BHT and WHT by Reservoir Simulation and Analytical Methods. Two steamflood areas will be discussed. Case 1a is for a 2008 steamflood commercial expansion project. Case 1b is for a 2012 steamflood expansion project. Case 1a is covered by a reservoir simulation study, which can be applied for comparison with the Lauwerier (1955) analytical model for BHT. Case 1b does not have a reservoir-simulation model, and only the analytical methods are available to forecast BHT and WHT using the FLT measurements. One of the most important operational parameters, the steam injection rate, was approximately 80 B/D in Case 1a before 2014 and was adjusted to an optimal rate of 45 to 60 B/D according to an integrated reservoir study and field surveillance investigation. This optimal steam injection rate is endorsed in future long-term BHT forecast in reservoir simulation. The WHT forecast generated by the steady-state wellbore model uses an average gross-production rate from field data, which is consistent with the optimal steam injection rate. Temperature is not a summation variable; therefore, all individual producers in those areas should follow the behavior.

Fig. 7 compares the Case 1a predicted BHT from a reservoir simulation and the Lauwerier (1955) model. With steam response time of 1.59 years as the only matching parameter in the Lauwerier (1955) model, the BHT is consistent with that from reservoir simulation. The higher BHT in the reservoir simulation before 2014 was attributed to the historically higher steam injection rate up to 80 B/D. A steam response time consistent with the optimal steam injection rate is used to predict BHT in the Lauwerier (1955) model, which generates a similar BHT response from reservoir simulation. It is straightforward to forecast the WHT in the Hasan et al. (2009) steady-state wellbore model. Fig. 7 also shows the WHT long-term forecast from the steady-state model as well as the monthly average FLT

measurements. The FLT measurement starts to be consistent with the WHT forecast when the optimal steam injection rate (45 to 60 B/D) is used, although the earlier FLT measurements are higher because of higher steam injection rates up to 80 B/D. Fig. 7 also shows a BHT/WHT crossover at approximately 180 to 200°F, which is qualitatively consistent with field observation and simulation results (Fig. 5) that a low-BHT waterflood fluid is heated in the wellbore and a high-BHT steamflood-producing fluid is cooled in the wellbore attributed to the formation-temperature profile (Fig. 2).

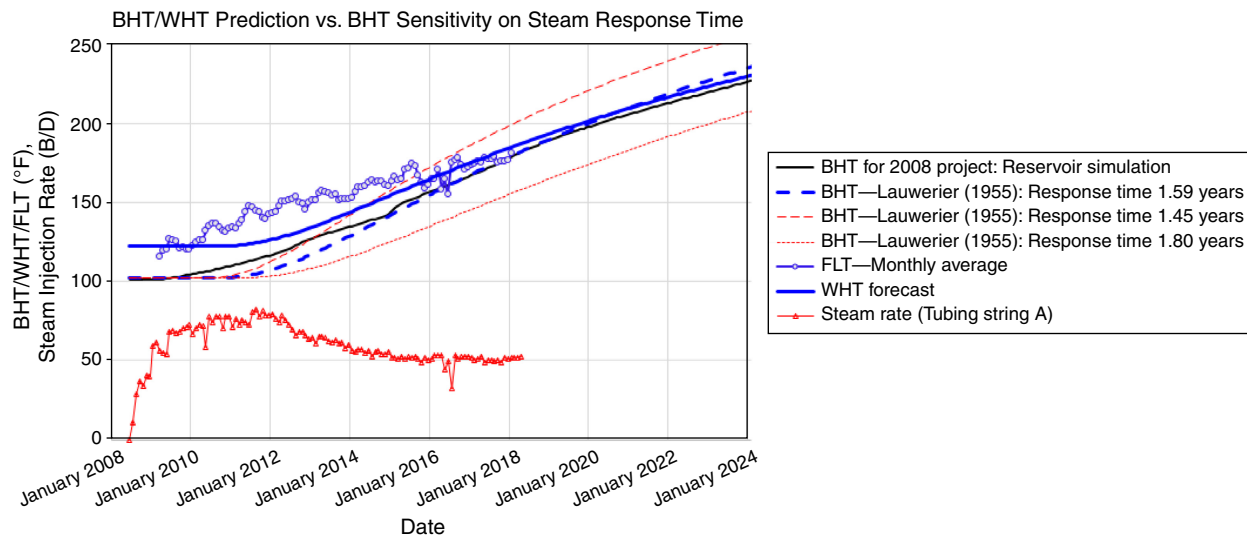


Fig. 7—Comparison of BHT from the reservoir simulation and the Lauwerier (1955) model for the 2008 project.

Case 1b does not have a reservoir-simulation model for predicting BHT. It will rely on analytical models and field FLT measurements to forecast BHT and WHT. **Fig. 8** shows the monthly average measured FLT, the BHT forecast by the Lauwerier (1955) model, and the WHT prediction by the steady-state wellbore model. A quantitative comparison between the predicted WHT and FLT measurements should only be performed in the summer months when the heat loss in the wellbore and surface flowline is minimal. Both BHT and WHT predictions are only process dependent and season independent. By adjusting the steam response time to 1.59 years in the Lauwerier (1955) model, the WHT predicted in the wellbore model is consistent with the FLT measurement in the summer months. With 5 years of FLT-measurement data to calibrate the steamflood response time, WHT can be predicted without reservoir simulation. This analytical approach provided a convenience for forecasting the WHT in steamflood operation. This WHT forecast will be useful for surface-facility design and can also be used as a production-performance diagnostic tool.

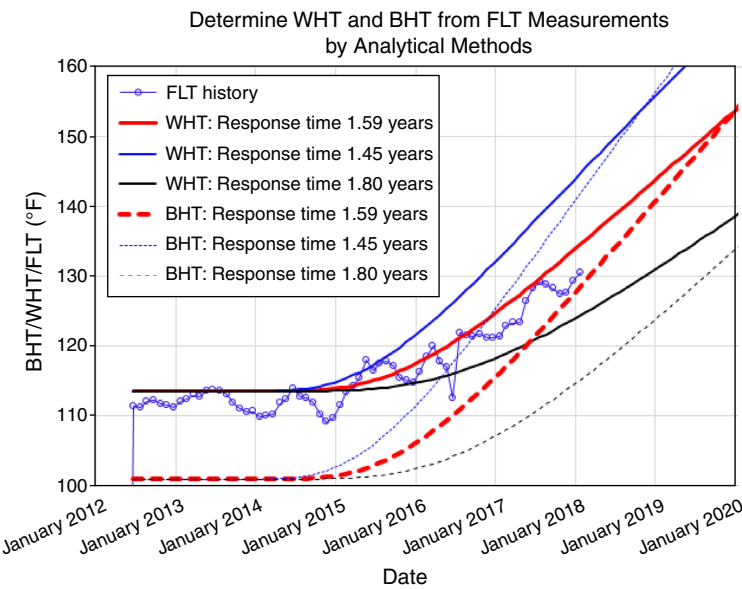


Fig. 8—Determine WHT and BHT from FLT measurements by analytical methods.

Case 2: Diagnose Possible Operational Issues to Steamflood Performance. Two major possible operational issues affecting steamflood production performance in South Belridge Diatomite are premature steam breakthrough ("hot" producer) and water channeling ("cold" producer) on the waterflood/steamflood boundary. The Y -function method can be applied to qualitatively diagnose the steamflood displacement efficiency reduction caused by water or steam channeling from the dramatic drop in oil cut or Y -function. However, the Y -function method cannot tell premature steam breakthrough from water channeling, which can be clarified by integrated application of the Y -function method with the WHT prediction and FLT measurements.

Case 2a: Diagnose “Hot” Producer Using Premature Steam Breakthrough. A “hot” producer sees rapidly increasing FLT measurement, which is generally caused by abnormal premature steam breakthrough from an induced fracture rather than normal displacement. Producer 964LR-33 is applied to demonstrate both the early normal steamflood performance and the late “hot” producer issue when premature steam breakthrough occurs. **Fig. 9** shows the Y-function analysis for the positive oil banking above the -1 slope waterflood trend before July 2015, which is an expected normal behavior for a steamflood diatomite producer. A significant abnormal reduction in oil cut and Y-function can be observed after July 2015, which is an operational issue that needs to be diagnosed. **Fig. 10** compares the WHT forecast and the FLT measurement. The WHT forecast for the entire period and the measured FLT before July 2015 are the expected temperature-behavior signal for a normal steamflood response. After July 2015, the FLT temperature increases rapidly to 250°F and surpasses the WHT for a normal steamflood expectation of 150 to 170°F during the period. Therefore, this producer became a “hot” producer from this point on. It can be observed that it took nearly 6 months to reach the maximum temperature of 250°F as well as see the loss of oil production. This 6-month alert period provides an opportunity to diagnose the operational problem and take the appropriate measure to overcome the operational issue before it gets worse and causes oil-production loss. Comparing predicted WHT with measured FLT will diagnose a “hot” producer but cannot predict the high flat FLT after premature steam breakthrough, which is related to the operational action in choking a “hot” producer to prevent vapor production.

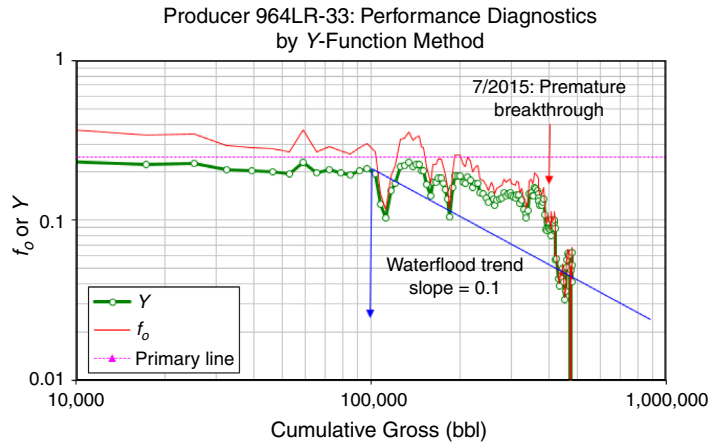


Fig. 9—Y-function representation of the waterflood and steamflood production performance.

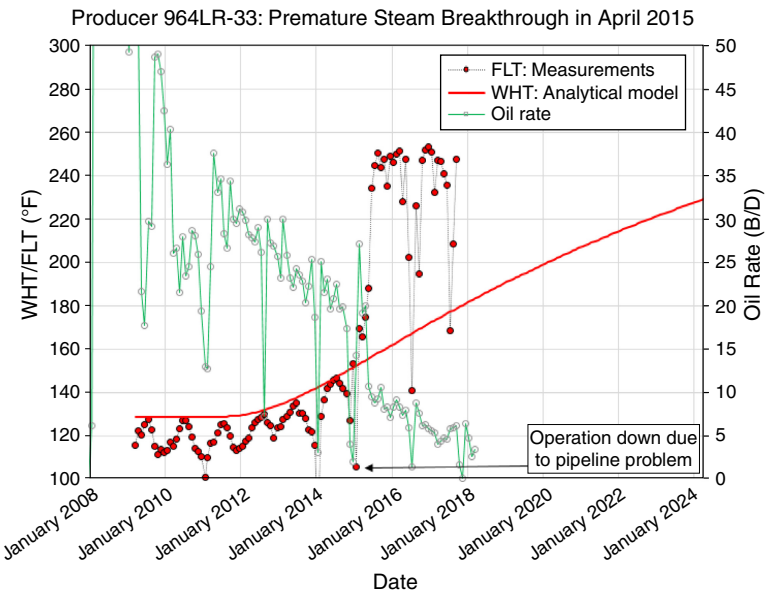


Fig. 10—Producer 964LR-33: Premature steam breakthrough and its effect on oil production.

Upon confirming the premature steam breakthrough into the producer from the WHT and FLT comparisons, which is manifested in an oil-rate loss (Fig. 10) and a dramatic displacement-efficiency reduction shown by the oil cut in the Y-function method (Fig. 9), the next step is to detect the steam injector(s) linking to the producer and causing the premature steam breakthrough. A producer-centered pattern approach is recommended. **Fig. 11** shows the steamflood pattern centered by Producer 964LR-33, with the straight lines denoting the induced fracture orientation described by surface tilt-meter measurements at the time of the hydraulic-fracture job. Generally speaking, the more likely steam-channeling direction is in the north/south direction because of the fracture-orientation closeness between the injector(s) and the producer, although the possibility cannot be excluded that the injectors on the east/west orientation might cause the problem. **Fig. 12** correlates the timing of all the steam injection-pressure events with the abnormal dramatic FLT increases on the center Producer 964LR-33 for detecting the direction of steam channeling. It is evident that the communication was from the steam injection strings, Strings 765EURC-33 and 765EURD-33, where injection pressure was equalized and caused premature

steam breakthrough into Producer 964LR-33 in the shallower D cycle. This example demonstrates that a routinely available surface operational parameter, such as abnormal steam breakthrough, can be diagnosed for the interval and orientation, as well as the level of damage, to provide a basis for possible remediation work. Solutions for this kind of operational problem through repairing either or both the injectors and producer in the breakthrough intervals are being investigated for overcoming the damage caused.

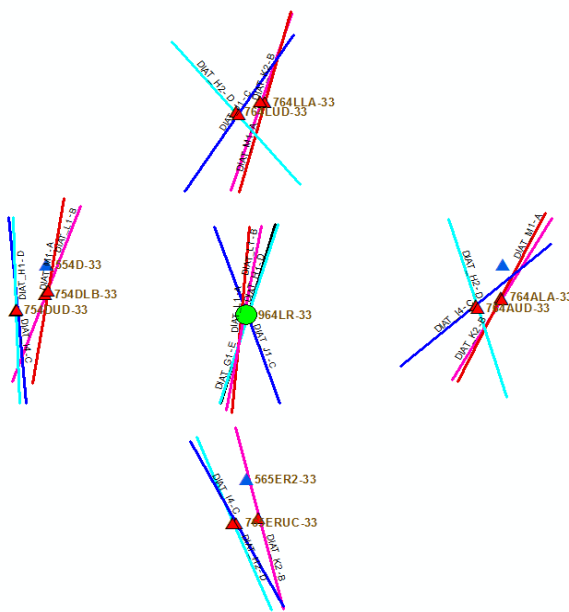


Fig. 11—Pattern centered by Producer 964LR-33 and surrounding steam injectors.

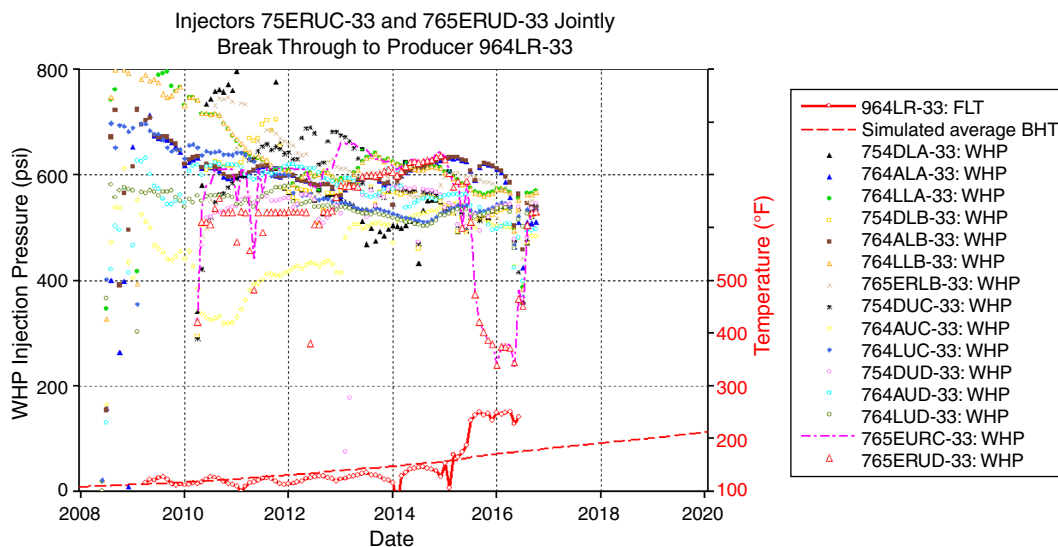


Fig. 12—South Injectors 765ERUC-33 and 765ERUD-33 jointly break through to the producer.

Case 2b: Diagnose “Cold” Producer Using Interactions with Water Injectors. The South Belridge Diatomite steamflood was developed after the original waterflood development. Some flank area remains at waterflood because of unsuitable reservoir quality for steamflood operations (such as thickness or oil saturation). The top G interval remains on water injection, whereas the four lower conformance intervals referred to as A through D are on steam injection, and all producers are designed as commingled across all five intervals (**Fig. 13**). As a result, most producers’ gross and oil production should contain a small waterflood-performance element in G intervals, whereas the producers on the steamflood/waterflood boundary might be influenced more by the remaining full-interval water injection in the flank area. Appropriate water injection rate target control is important in those boundary steamflood producers to avoid water channeling and to minimize interference by water injection.

Producer 941F-33 is near the steamflood/waterflood boundary, as shown in **Fig. 13**, in a producer-centered pattern with steam injectors and three surrounding water injectors: 541CR2-33 (G interval only), 541GRS-33 (G, D, and C intervals), and 541GR3L-33 (B and A intervals). **Fig. 14** shows the oil cut and Y-function diagnostic analysis (Yang 2012). There are seven significant milestones to production performance in **Fig. 14** and three water-channeling periods that are verified by WHT/FLT comparison. The producer started with primary production with higher oil cut (approximately 0.5) and nearly constant Y value of 0.25. The first water channeling started at time T_1 = July 2005 and terminated at time T_2 = January 2007, when water injectors were shut in for conversion to steam injection at time T_3 = January 2009. A significant reduction in f_o and Y values can be observed during water channeling. The f_o and Y values

increase significantly during steamflood development (January 2007 to January 2009) because of discontinuing water channeling and the steamflood oil-banking effect. The second water-channeling events occurred at time T_4 = June 2012 with the dramatically decreasing f_o and Y values. This water-channeling effect was minimized from time T_5 = March 2014 by the oil-banking effect, with the steamflood maturing as indicated by increasing FLT (Fig. 15). The third water-channeling period started at time T_6 = April 2016 and lasted to the date of this study. At T_7 = August 2017, there was a fieldwide Voidage-management action and the Producer 941F-33 pump was constrained to reduce gross production. All three premature-breakthrough periods can be verified as water channeling rather than steam channeling after comparing the WHT prediction and FLT measurements, as shown in Fig. 15. A significant oil-productivity loss can be observed for the first (T_1 = July 2005 and T_2 = January 2007) and the third (after T_6 = April 2016) water-channeling periods.

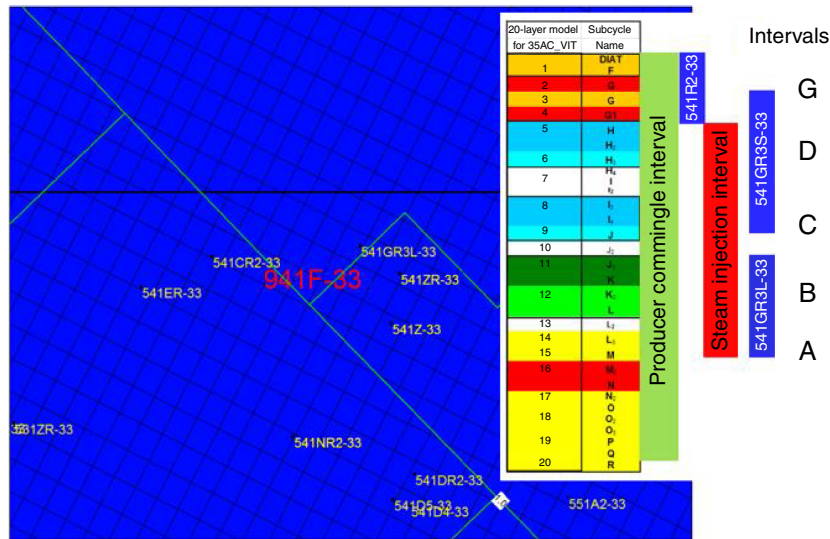


Fig. 13—Producer 941F-33 and surrounding active water injector with conformance intervals.

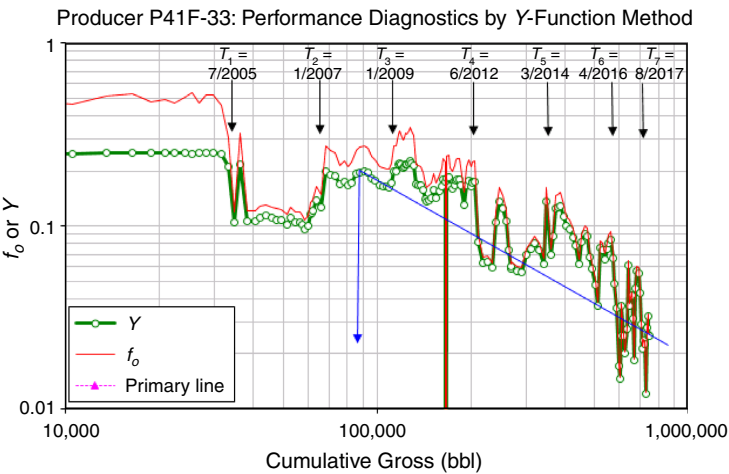


Fig. 14—Y-function diagnostics for Producer 941F-33.

Upon confirming water channeling using the Y-function method and WHT/FLT comparison, the subsequent task is to investigate the water injector(s) causing the water-channeling issue. Fig. 16 compares the WHT/FLT and the wellhead injection pressures (WHPs) for the G water Injector 541CR2-33 and both the flank “short” water Injector 541GR3S-33 (G, Dm and C intervals) and the “long” water Injector 541GR3L-33 (B and A intervals) with two water-channeling times (T_4 = June 2012 and T_6 = April 2016). There is no clear correlation between the water-channeling milestones T_4 and T_6 with the G water Injector 541CR2-33. The short Injector 541GR3S-33 saw an increasing WHP and then a 50-psi drop at time T_4 . Therefore, the water channeling at time T_4 = June 2016 was likely caused by the short Injector String 541GR3S-33. The water-channeling event at time T_6 = April 2016 could not be caused jointly with another surrounding injector, Injectors 541CR2-33 or 541GR3L-33, because their WHPs are not equalizing with the WHP of Injector 541GR3S-33. Confirmation is also indicated by the dramatic gross-production reduction from an average of 310 B/D to approximately 230 B/D starting from January 2016 (possibly caused by rod-pump-efficiency reduction). Under the unconstrained production period (before January 2016), the water channeling from Injector 541GR3S-33 with a 200-B/D target rate increases the gross production in Producer 941F-33 without significantly damaging the oil production from the steamflood contribution. When the producer is constrained by pumping-efficiency reduction, the oil and water phases compete for the limited lifting capacity and result in the oil-production loss caused by unfavorable mobility. From this diagnostic analysis, we learned that an inappropriate injection-rate target can cause a water-channeling issue. To recover the oil-production capacity from Producer 941F-33, a recommended resolution is to shut in the Injector String 543GR3S-33 because water injection in this water-channeling source injector does not efficiently contribute to the oil production in Producer 941F-33.

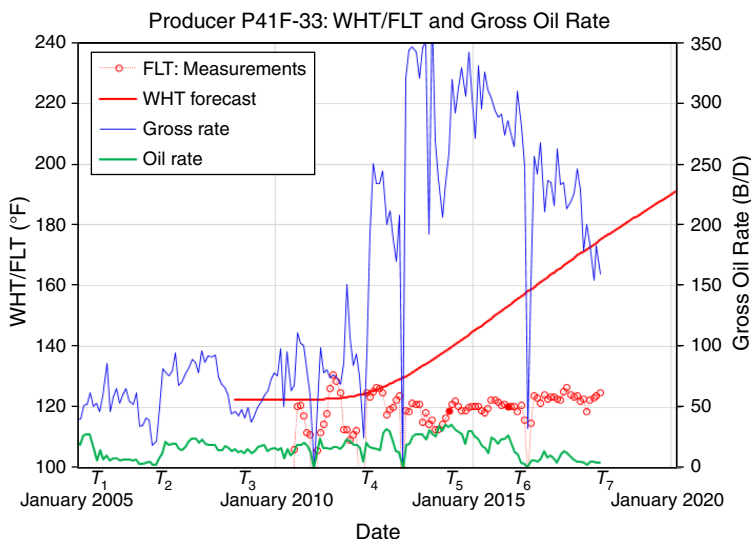


Fig. 15—WHT/FLT diagnosis indicates “cold” producer.

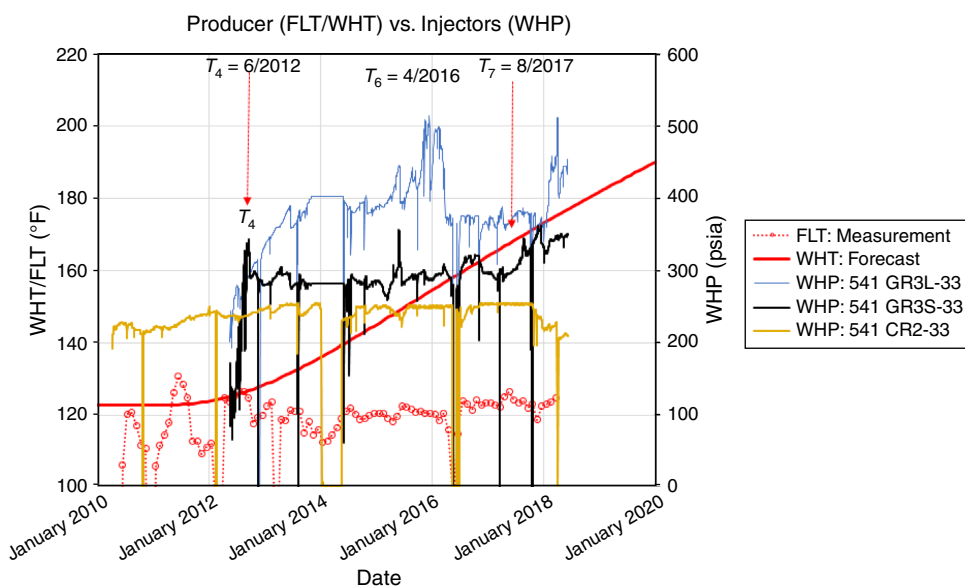


Fig. 16—Diagnose the water injector causing the water channeling into Producer 941F-33.

Conclusions

An integrated analytical approach is proposed to predict BHTs for steamflood producers from the Lauwerier (1955) convective/conductive heat-transfer model and then predict the producer WHT from a steady-state wellbore model with multiple temperature-gradient sections (Hasan et al. 2009). WHT can be verified as a linear relationship with the BHT, with slope and intercept as the functions of the gross-production rate. The predicted WHT can be related to the summer month (in general, July through September) FLT measurements on a monthly average basis. The field case study of the South Belridge Diatomite steamflood demonstrates that the BHT from reservoir-simulation results can be applied to calibrate the Lauwerier (1955) model for the steam response time, and we then apply the steady-state wellbore model to forecast the WHT. On the other hand, when a reservoir-simulation model does not exist, several years of FLT measurement during the steamflood are necessary to calibrate the WHT to predict the BHT and WHT in the analytical model. The WHT forecast can be used to help design steamflood surface facilities. In addition, the WHT forecast and monthly averaged FLT measurements can be applied to production-performance monitoring to help diagnose possible steam/water-channeling issues by integrating the displacement-efficiency analysis using the Y -function method and the thermal behavior in the WHT/BHT predictions. The analysis and field case study demonstrate that with only surface measurements of FLT, the oil- and water-rate measurements, and the surface-injection rate/pressure signals, steamflood production performance can be diagnosed for operational issues intended for proposing remediation actions to optimize the production performance.

Nomenclature

A = slope constant

b = half-formation thickness, $b = 1$ ft

B = relative permeability ratio constant, intercept constant

c = heat capacity, Btu/lbm-°F

c_p = specific heat capacity of fluid, Btu/lbm-°F
 D = depth, ft
 E_V = volumetric sweep efficiency
 f = fractional flow
 g_G = formation-temperature gradient, °F/ft
 k = thermal conductivity, Btu/D-ft-°F
 k_r = relative permeability
 L_R = relaxation parameter to steady state (Eq. B-16); see Hasan et al. (2009)
 PV = pore volume, bbl
 Q_L = cumulative gross production, bbl
 r_{to} = outside tubing radius, in.
 r_w = wellbore radius, ft
 S = saturation
 t = time, days
 t_D = dimensionless time
 T = temperature, °F
 T_D = dimensionless temperature
 T_e = initial formation temperature
 T_r = reservoir temperature, °F
 T_s = steam temperature, °F
 U_{to} = overall heat-transfer coefficients, Btu/(hr-ft²-°F)
 w = mass rate, lbm/hr
 x = distance from injector, ft
 $Y = f_o(1-f_o)$, Y-function
 z = depth, ft
 α_E = thermal diffusivity
 θ = heat-capacity ratio between formation and overburden
 λ = thermal conductivity, Btu/D-ft-°F
 ν_w = linear water velocity, ft/yr
 ξ = dimensionless distance
 ρ = density, g/cm³
 τ = dimensionless time
 ϕ = porosity

Subscripts

1 = formation
 2 = overburden and underburden
 BH = bottomhole
 L = liquid (oil + water)
 o = oil
 w = water
 WH = wellhead

Acknowledgments

The author would like to thank Aera Energy LLC for the permission to publish this work.

References

- Dietrich, J. 1990. Steamflooding in a Waterdrive Reservoir: Upper Tulare Sands, South Belridge Field. *SPE Res Eval & Eng* **5** (3): 275–284. SPE-17453-PA. <https://doi.org/10.2118/17453-PA>.
- Gwadera, M., Larwa, B., and Kupiec, K. 2017. Undisturbed Ground Temperature—Different Methods of Determination. *Sustainability* **9** (11): 1–14. <https://doi.org/10.3390/su9112055>.
- Hasan, A. R., Kabir, C. S., and Wang, X. 2009. A Robust Steady-State Model for Flowing Fluid Temperature in Complex Wells. *SPE Prod & Oper* **24** (2): 269–276. SPE-109765-PA. <https://doi.org/10.2118/109765-PA>.
- Hong, K. C. 1994. *Steamflood Reservoir Management: Thermal Enhanced Oil Recovery*. Tulsa, Oklahoma, USA: PennWell Books.
- Izgec, B., Hasan, A. R., Lin, D. et al. 2010. Flow-Rate Estimation from Wellhead-Pressure and Temperature Data. *SPE Prod & Oper* **25** (1): 31–39. SPE-115790-PA. <https://doi.org/10.2118/115790-PA>.
- Lauwerier, H. A. 1955. The Transport of Heat in an Oil Layer Caused by the Injection of Hot Fluid. *Appl. Sci. Res. A* **5**: 145–150. <https://doi.org/10.1007/BF03184614>.
- Marx, J. W. and Langenheim, R. H. 1959. Reservoir Heating by Hot Fluid Injection. SPE-1266-G.
- Nath, D. K., Sugianto, R., and Finley, D. B. 2007. Fiber-Optic Distributed Temperature Sensing Technology Used for Reservoir Monitoring in an Indonesia Steam Flood. *SPE Drill & Compl* **22** (2): 149–156. SPE-97912-PA. <https://doi.org/10.2118/97912-PA>.
- Neuman, C. H. 1985. A Gravity Override Model of the Steamdrive. *J Pet Technol* **37** (1): 163–169. SPE-13348-PA. <https://doi.org/10.2118/13348-PA>.
- Qi, Q., Pepin, S., Al Jazaf, A. et al. 2017. Errors Associated with Waterflood Monitoring Using the Hall Plot for Stacked Reservoirs in the Absence of Profile Surveys. Paper presented at the SPE Western Regional Meeting, Bakersfield, California, USA, 23–27 April. SPE-185694-MS. <https://doi.org/10.2118/185694-MS>.
- Ramey, H. J. Jr. 1962. Wellbore Heat Transmission. *J Pet Technol* **14** (4): 427–435. SPE-96-PA. <https://doi.org/10.2118/96-PA>.
- Saeid, S. and Barends, F. B. J. 2009. An Extension of Lauwerier's Solution for Heat Flow in Saturated Porous Media. Oral presentation given at the COMSOL Conference, Milan, Italy, 14–16 October.

- Silin, D. B., Holtzman, R., Patzek, T. W. et al. 2005. Waterflood Surveillance and Control: Incorporation Hall Plot and Slope Analysis. Paper presented at the SPE Annual Technical Conference and Exhibition, Dallas, Texas, USA, 9–12 October. SPE-95685-MS. <https://doi.org/10.2118/95685-MS>.
- Yang, Z. 2009. A New Diagnostic Analysis Method for Water Performance. *SPE Res Eval & Eng* **12** (2): 341–351. SPE-113856-PA. <https://doi.org/10.2118/113856-PA>.
- Yang, Z. M. 2012. Production-Performance Diagnostics Using Field-Production Data and Analytical Models: Method and Case Study for the Hydraulically Fractured South Belridge Diatomite. *SPE Res Eval & Eng* **15** (6): 712–724. SPE-153138-PA. <https://doi.org/10.2118/153138-PA>.
- Yang, Z. M. and Urdaneta, A. 2017. A Practical Approach to History Matching Premature Water Breakthrough in Waterflood Reservoir Simulation: Method and Case Studies in South Belridge Diatomite Waterflood. *SPE Res Eval & Eng* **20** (3): 726–737. SPE-174006-PA. <https://doi.org/10.2118/174006-PA>.

Appendix A—Predicting Steamflood BHT with the Lauwerier (1955) Convective/Conductive Formation-Heat-Transport Model

Lauwerier (1955) proposed a convective/conductive heat-transport model in 2D and a two-layer formation, as shown in Fig. 3:

$$b\rho_1 c_1 \frac{\partial T_1}{\partial t} + b\rho_w c_w v_w \frac{\partial T_1}{\partial x} - \lambda_2 \left(\frac{\partial T_2}{\partial z} \right)_{z=b} = 0, \quad \dots \quad (A-1)$$

$$\lambda_2 \frac{\partial^2 T_2}{\partial z^2} = \rho_2 c_2 \frac{\partial T_2}{\partial t}, \quad \dots \quad (A-2)$$

Layer 1 (thickness $2b$, $|z| < b$) represents the formation and Layer 2 ($|z| > b$) represents the overburden and underburden. Major assumptions include a uniform formation-temperature profile in Layer 1; only longitudinal formation-heat convection in Layer 1; and only heat conduction in the vertical direction in the overburden and underburden in Layer 2. It is appropriate to clarify that by specifying the linear water velocity v_w in the formation (Layer 1) and assuming a uniform temperature profile in the vertical direction rather than specifying an actual volumetric injection rate and formation thickness as well as volumetric sweeping efficiency for defining the heat front, the half-formation thickness (b) in the heat-transport equation is equal to unity ($b = 1$). The dimensionless formation temperature from the analytical solution is

$$\frac{T_1 - T_r}{T_s - T_r} = \operatorname{erfc} \left[\frac{\xi}{2\sqrt{\theta(\tau - \xi)}} \right] U[\tau - \xi], \quad \dots \quad (A-3)$$

where T_1 is formation temperature, T_s is steam temperature, and T_r is the formation initial temperature. Time τ , distance ξ , and heat-capacity ratio between formation and overburden θ , all dimensionless, are defined in **Table A-1**. The complementary error function can be approximated by

$$\operatorname{erfc}(x) = 1.3693e^{-0.8072(x+0.6382)^2}. \quad \dots \quad (A-4)$$

| Variable | Value or Variable Composite | Field Unit |
|-----------|---|---------------|
| x | 107.5, (orientation, 22.5° north/east) | ft |
| v_w | x/t_s | ft/yr |
| θ | $= (\rho_1 c_1)/(\rho_2 c_2)$ | Dimensionless |
| τ | $\tau = \lambda_2 t/(b^2 \rho_1 c_1) = 0.023406 \lambda_2 t/[b^2]t$ | Dimensionless |
| ξ | $\xi = x \lambda_2 / (b^2 \rho_w c_w v_w) = 5.853132 x \lambda_2 / [b^2 v_w]$ | Dimensionless |
| T_s | 550 | °F |
| T_r | 105 | °F |
| λ | 3.5 | Btu/D-ft-°F |
| ϕ | 0.55 | Dimensionless |
| ρ_w | 62.43 | lbm/ft³ |
| ρ_o | 55.039 | lbm/ft³ |
| ρ_L | $= f_w \rho_w + (1-f_w) \rho_o = 61.321$ | lbm/ft³ |
| ρ_s | 139.21 | lbm/ft³ |
| c_w | 0.999 | Btu/lbm-ft-°F |
| c_o | 0.51 | Btu/lbm-ft-°F |
| c_s | 0.21 | Btu/lbm-ft-°F |
| c_L | 0.9257 | Btu/lbm-ft-°F |
| S_{wc} | 0.50 (connate-water saturation) | |
| S_{orw} | 0.25 (residual oil saturation) | |

Table A-1—Key parameters for the Lauwerier (1955) model (South Belridge Diatomite Field).

To better represent the Lauwerier (1955) model to the field BHT, a history match to an earlier temperature history by adjusting the linear velocity or time to response is necessary. There are two history-match scenarios: match the BHT from the Lauwerier (1955) model to the reservoir-simulation result when the reservoir-simulation model is available, or calculate WHT from BHT in the Lauwerier (1955) model by adjusting the response time and matching with several years of earlier FWT data.

Table A-1 shows the key parameters to the Lauwerier (1955) model and the basic reservoir and fluid properties for the South Belridge Diatomite Field.

Appendix B—Model WHT from BHT Using the Steady-State Wellbore Model (Hasan et al. 2009)

Hasan et al. (2009) proposed a steady-state wellbore model for both injectors and producers with multiple wellbore inclinations or geothermal sections, specifically for flowing wells with considerations of the potential (gravity), kinetic-energy, and Joule-Thompson expansion effects in the isothermal primary depletion wells. For a vertical wellbore in a multisection geothermal-trend formation with liquid-phase production, the kinetic-energy and Joule-Thompson effects might be neglected (Ramey 1962) or compensate each other with the relatively shallow depth and low liquid-production rate; therefore,

$$\frac{dT_f}{dz} = L_R(T_f - T_e), \quad \dots \dots \dots \quad (\text{B-1})$$

where L_R is the total heat-transfer coefficient. The formation temperature T_{ej} in the j th geothermal section is dependent on depth z and geothermal gradient g_{Gj} ,

$$T_{ej} = T_e + g_{Gj}(z_j - z), \quad \dots \dots \dots \quad (\text{B-2})$$

where T_e is the formation temperature at the top depth z . The fluid-temperature profile T_f in a producer wellbore is solved in Eq. B-3, where the subscript j indicates the entrance to the geothermal-trend section in a bottom-up computational sequence.

$$T_f = T_e + \frac{1 - e^{(z-z_j)L_R}}{L_R} g_{Gj} + e^{(z-z_j)L_R} (T_{fj} - T_{ej}). \quad \dots \dots \dots \quad (\text{B-3})$$

Simple Geothermal Gradient. For the simple case of a vertical well with one geothermal section, in Eq. B-3 we have $z=0$, $z_j=D$ (formation depth), $T_e=T_{eWH}$, $T_{fj}=T_{fBH}$, and $T_{ej}=T_{eBH}$. The WHT is

$$T_{fWH} = e^{-DL_R} T_{fBH} + \left(T_{eWH} - T_{eBHE}^{-DL_R} + \frac{1 - e^{-DL_R}}{L_R} g_G \right), \quad \dots \dots \dots \quad (\text{B-4a})$$

which indicates a linear relationship of $T_{fWH} = A_1 T_{fBH} + B_1$ between the WHT and the BHT, with slope A_1 and intercept B_1 as

$$A_1 = e^{-D/L_R}, \quad \dots \dots \dots \quad (\text{B-4b})$$

$$B_1 = T_{eWH} - T_{eBHE}^{-DL_R} + \frac{1 - e^{-DL_R}}{L_R} g_G. \quad \dots \dots \dots \quad (\text{B-4c})$$

BHT can be predicted using the Lauwerier (1955) analytical model or from reservoir simulation.

Three-Temperature-Gradient Section. The three-section geothermal description in South Belridge Diatomite Field is shown in Fig. 3. For the third section (between z_2 and bottomhole $z=D$), the equivalent formation temperature gradient $g_{G3}=0$; thus,

$$T_f = T_e + e^{(z-D)L_R} (T_{fBH} - T_{eBH}). \quad \dots \dots \dots \quad (\text{B-5})$$

At bottomhole depth ($z=D$),

$$T_f = T_{fBH}. \quad \dots \dots \dots \quad (\text{B-6})$$

At depth z_2 ,

$$T_{f2} = T_{eBH} + e^{(z_2-D)L_R} (T_{fBH} - T_{eBH}). \quad \dots \dots \dots \quad (\text{B-7})$$

For the second section (between z_1 and z_2),

$$T_f = T_e + \frac{1 - e^{(z-z_2)L_R}}{L_R} g_{G2} + e^{(z-z_2)L_R} (T_{f2} - T_{eBH}). \quad \dots \dots \dots \quad (\text{B-8})$$

At depth z_1 ,

$$T_{f1} = T_{e1} + \frac{1 - e^{(z_1-z_2)L_R}}{L_R} g_{G1} + e^{(z_1-z_2)L_R} (T_{f2} - T_{eBH}). \quad \dots \dots \dots \quad (\text{B-9})$$

For the first section (between wellhead $z=0$ and z_1),

$$T_f = T_e + \frac{1 - e^{(z-z_1)L_R}}{L_R} g_{G1} + e^{(z-z_1)L_R} (T_{f1} - T_{e1}), \quad \dots \dots \dots \quad (\text{B-10})$$

with

At wellhead $z=0$, we have

Substituting T_{f2} in Eq. B-7 into T_{f1} Eq. B-9 and then substituting T_{f1} into Eq. B-10 for T_{fWH} , a linear relationship is obtained with slope A and intercept B dependent on flow rate through total heat-transfer coefficient L_R ,

with

$$B = T_{eWH} - T_{eBH} e^{-DL_R} + \frac{1 - e^{-z1L_R}}{L_R} g_{G1} + \frac{e^{-z1L_R} - e^{-z2L_R}}{L_R} g_{G2}, \quad \dots \dots \dots \quad (\text{B-15})$$

and

Zhengming Yang is a senior staff reservoir engineer with Aera Energy LLC, a Shell and ExxonMobil joint venture, in Bakersfield, California, USA. He works on integrated reservoir study and simulation projects, as well as performance diagnosis and forecasts from field-production data. Yang holds a diploma in chemical engineering from Tianjin University in Tianjin, China; a master's degree in petroleum engineering from the Research Institute of Petroleum Exploration and Development, China; and a PhD degree in petroleum engineering from the University of Southern California.